A time domain finite-difference technique for oblique incidence of antiplane waves in heterogeneous dissipative media

Arrigo Caserta
Istituto Nazionale di Geofisica, Roma, Italy

Abstract
This paper deals with the antiplane wave propagation in a 2D heterogeneous dissipative medium with complex layer interfaces and irregular topography. The initial boundary value problem which represents the viscoelastic dynamics driving 2D antiplane wave propagation is formulated. The discretization scheme is based on the finite-difference technique. Our approach presents some innovative features. First, the introduction of the forcing term into the equation of motion offers the advantage of an easier handling of different inputs such as general functions of spatial coordinates and time. Second, in the case of a straight-line source, the symmetry of the incident plane wave allows us to solve the problem of oblique incidence simply by rotating the 2D model. This artifice reduces the oblique incidence to the vertical one. Third, the conventional rheological model of the generalized Maxwell body has been extended to include the stress-free boundary condition. For this reason we solve explicitly the stress-free boundary condition, not following the most popular technique called *vacuum formalism*. Finally, our numerical code has been constructed to model the seismic response of complex geological structures: real geological interfaces are automatically digitized and easily introduced in the input model. Three numerical applications are discussed. To validate our numerical model, the first test compares the results of our code with others shown in the literature. The second application rotates the input model to simulate the oblique incidence. The third one deals with a real high-complexity 2D geological structure.

Key words *seismic wave propagation – numerical method – dissipative media*

1. Introduction

The numerical approach is a necessary tool to investigate wave propagation in heterogeneous media. The available numerical methods are mainly based on boundary techniques or domain techniques (Bard, 1995). The former are such as boundary integrals (*e.g.* Sánchez-Sesma and Campillo, 1991) or discrete-wavenumber (*e.g.* Bard and Bouchon, 1980); the latter are such as finite-elements (*e.g.* Padovani *et al.*, 1995) or finite-differences (*e.g.* Moczo, 1989; Zahradnik *et al.*, 1993).

As far as the finite-difference technique is concerned, many computer codes are available nowadays. Moczo (1989) first used a finite-difference scheme with a variable grid, Moczo and Bard (1993) generalized the Emmerik and Korn (1987) rheological model to the heterogenous media, Zahradnik *et al.* (1993) tested four finite-difference schemes to better stabilize the solution.

The main goal of this paper is to set up a numerical technique suited to deal with complex geological interfaces necessary for applications to real structures, both for vertical and oblique incidence. An original scheme, based on the finite-difference technique, is presented. It is particularly oriented to studies of seismo-

Mailing address: Dr. Arrigo Caserta, Istituto Nazionale di Geofisica, Via di Vigna Murata 605, 00143 Roma, Italy; e-mail: caserta@ing750.ingrm.it

logical and engineering interest. The numerical computation of ground motion for realistic 2D nearsurface structures is performed for the antiplane component of the wavefield. This scheme is aimed to provide synthetic ground motion for plane waves obliquely incident to the bedrock. To reproduce realistic layered structures, the input model is provided by digitization of the real geological interfaces.

2. The model

The first step is to mathematically define the heterogeneous medium. Let $\Re^2$ be the two dimensional real space and $\underline{x} = (x, z) \in \Re^2$ a generic vector. With reference to fig. 1, let $f(x)$ be a regular function defined for $x \in \Re$ and let

$$\Omega = \{(x, z) \in \Re^2 \,|\, z > f(x),\ x \in \Re\}.$$

We denote with

$$\partial\Omega = \{(x, z) \in \Re^2 \,|\, z = f(x),\ x \in \Re\}$$

the boundary of Ω. The medium is modelled through the domain Ω, so that $\partial\Omega$ is the curve which separates the medium from the air. Let $\theta(\underline{x})$ be the angle between the outward vector normal to $\partial\Omega$, in the point $\underline{x} \in \partial\Omega$ and the positive real x axis. The medium is characterized by the following functions defined for $\underline{x} \in \Omega$: $\rho(\underline{x})$ the mass density per unit volume, $\mu_U(\underline{x})$ the unrelaxed shear modulus and $Q(\underline{x})$ the quality factor. The unknown functions are: $u(\underline{x}, t)$ that is the y displacement component and the auxiliary unknown functions $\xi_j(\underline{x}, t)$ and $\Psi_j(\underline{x}, t)$ $j = 1, 2, \cdots, p$ which take into account for absorption properties in Ω and on $\partial\Omega$ respectively.

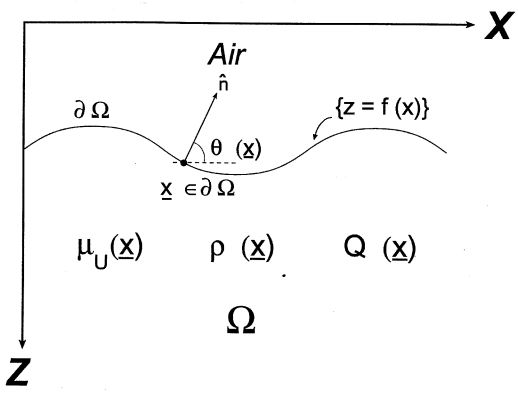

Fig. 1. Sketch of the integration domain for the initial boundary value problem (2.9) through (2.12). It represents the mathematical scheme of a heterogeneous unbounded medium Ω with free surface $\partial\Omega$. The density ρ, the quality factor Q and the shear modulus μ_U are functions of the spatial coordinates. The free surface $\partial\Omega$ is characterized by a function of x such as $\partial\Omega = \{z \in \Re \,|\, z = f(x)\}$.

The antiplane wave propagation is described by the following equation of motion:

$$\rho\frac{\partial^2 u}{\partial t^2} = \frac{\partial \sigma_{yx}}{\partial x} + \frac{\partial \sigma_{yz}}{\partial z} + G(\underline{x}, t) \qquad (2.1)$$

where σ_{yx} and σ_{yz} are the two relevant components of the stress tensor and $G(\underline{x}, t)$ is the forcing term.

To incorporate an attenuation law into a time-domain method, we adopt the rheological model of generalized Maxwell body of Emmerich and Korn (1987) as generalized by Moczo and Bard (1993) for heterogeneous media. The auxiliary unknown functions $\xi_j(\underline{x}, t)$ are solutions of the following system of equations (see Appendix):

$$\frac{\partial \xi_j}{\partial t} + \omega_j \xi_j = \omega_j \left[\frac{\partial}{\partial x}\left(\frac{\mu_U Y_j}{(1 + \sum_{j=1}^{p} Y_j)} \frac{\partial u}{\partial x} \right) + \right.$$

$$\left. + \frac{\partial}{\partial z}\left(\frac{\mu_U Y_j}{(1 + \sum_{j=1}^{p} Y_j)} \frac{\partial u}{\partial z} \right) \right] \qquad (2.2)$$

$$j = 1, 2, \cdots, p$$

where ω_j are the relaxation frequencies and the coefficients Y_j $j = 1, 2, \cdots, p$ are the weight factors of the classical Maxwell bodies constituting the generalized Maxwell body; they are the solutions of the linear system (A.3) in the Ap-

pendix. Formal differences between the definition of ξ_j, in (2.2), and the corresponding one in the paper by Moczo and Bard (1993) are due to the different approaches in the construction of the two finite-difference schemes. The relation between ξ_j in (2.2) and the same quantity ξ_j^{EK} in Emmerich and Korn (1987) is

$$\xi_j = \mu_U \xi_j^{EK}. \tag{2.3}$$

If the medium is homogeneous, replacing (2.3) in (A.5), eq. (2.2) is equal to (28) of Emmerich and Korn (1987).

The solutions of partial differential equations are not unique unless appropriate initial and boundary conditions are specified. In our problem the initial conditions are chosen to be zero and the initial perturbation is given by a forcing term, *i.e.* the function $G(\underline{x}, t)$ in eq. (2.1). On the surface $\partial\Omega$ we apply the stress-free boundary condition

$$\sigma_{y,n} = \sigma_{yx} \cos\theta + \sigma_{yz} \sin\theta = 0 \tag{2.4}$$

where $\sigma_{y,n}$ is the projection of the tangential stress on the normal outward direction on $\partial\Omega$, and θ is the angle between the outward normal vector to $\partial\Omega$ in $\underline{x} \in \partial\Omega$ and the positive x axis (see fig. 1). The physical meaning of (2.4) is that the surface can oscillate in order to maintain the normal projection of the tangential stress equal to zero at each time. In terms of displacement and in absence of absorption we have

$$\frac{\partial u}{\partial x} \cos\theta + \frac{\partial u}{\partial z} \sin\theta = 0. \tag{2.5}$$

Equation (2.5) can be also interpreted as the continuity of the traction across the interface between the medium and the vacuum. This point of view was recommended in the *SH* case by Boore (1972) suggesting therefore no need to explicitly approximate eq. (2.5). Zahradnik *et al.* (1993) refer to it as the *vacuum formalism*: the free-surface is formally manipulated in the same way as the internal points. Justification for this comes from the fact that in the discretized equation of motion an additional body-force term automatically appears, which guarantees the traction continuity. For details see Zahradnik and Priolo (1995) and Zahradnik (1995).

In order to mathematically represent the wave propagation in dissipative media and to include absorption on the free surface, it is better to maintain the distinction between the initial conditions, boundary conditions and equations of motion. Thus, we will solve eq. (2.5) explicitly.

We introduce absorption also in the stress-free boundary condition. The stress-free boundary conditions in absence of absorption are expressed by eq. (2.4). In the viscoelastic medium the components of tangential stress σ_{yx} and σ_{yz} are expressed by eq. (A.1). Therefore, substituting (A.1) in (2.4) we get

$$\frac{\partial u}{\partial x} \cos\theta + \frac{\partial u}{\partial z} \sin\theta - 2 \sum_{j=1}^{p} \cdot \cdot (\zeta_{j,yx} \cos\theta + \zeta_{j,yz} \sin\theta) = 0. \tag{2.6}$$

We define new auxiliary unknown functions as

$$\Psi_j \equiv 2 (\zeta_{j,yx} \cos\theta + \zeta_{j,yz} \sin\theta),$$

and eq. (2.6) becomes

$$\frac{\partial u}{\partial x} \cos\theta + \frac{\partial u}{\partial z} \sin\theta - \sum_{j=1}^{p} \Psi_j = 0. \tag{2.7}$$

The absorption tensors $\zeta_{j,yx}$ and $\zeta_{j,yz}$ obey the system of eqs. (A.2). In order to find the equations for Ψ_j. we multiply the first equation of (A.2) by $\cos\theta$ and the second one by $2 \sin\theta$. Summing them up we get

$$\frac{\partial \Psi_j}{\partial t} + 2\omega_j \Psi_j = = \frac{\omega_j Y_j}{1 + \sum_{j=1}^{p} Y_j} \left(\frac{\partial u}{\partial x} \cos\theta + \frac{\partial u}{\partial z} \sin\theta \right), \tag{2.8}$$

$$\forall (\underline{x}, t) \in \partial\Omega \times (0, \infty) \quad j = 1, 2, \cdots, p.$$

The partial differential eq. (2.7) coupled with the system of ordinary differential eq. (2.8) and

with initial conditions for Ψ_j $j = 1, 2, \cdots, p$ represents the *stress-free dissipative* boundary conditions, *i.e.* the stress-free boundary condition in the viscoelastic medium.

To summarize, our initial boundary value problem which mathematically represents the viscoelastic dynamics of antiplane wave propagation in 2D heterogeneous dissipative media is

$$\rho \frac{\partial^2 u}{\partial t^2} = \frac{\partial}{\partial x}\left(\mu_U \frac{\partial u}{\partial x}\right) + \frac{\partial}{\partial z}\left(\mu_U \frac{\partial u}{\partial z}\right) - \\ - \sum_{j=1}^{p} \xi_j (\underline{x}, t) + G(\underline{x}, t)$$

$$\forall (\underline{x}, t) \in \Omega \times (0, \infty) \qquad (2.9)$$

$$\frac{\partial \xi_j}{\partial t} + \omega_j \xi_j = \omega_j \left[\frac{\partial}{\partial x}\left(\frac{\mu_U Y_j (Q)}{1 + \sum_{j=1}^{p} Y_j (Q)} \frac{\partial u}{\partial x} \right) + \right.$$

$$\left. + \frac{\partial}{\partial z}\left(\frac{\mu_U Y_j (Q)}{1 + \sum_{j=1}^{p} Y_j (Q)} \frac{\partial u}{\partial z} \right) \right]$$

$$\forall (\underline{x}, t) \in \Omega \times (0, \infty) \quad j = 1, 2, \cdots, p \qquad (2.10)$$

$$\xi_j (\underline{x}, t = 0) = 0,$$

$$u (\underline{x}, t = 0) = 0, \qquad (2.11)$$

$$\frac{\partial u (\underline{x}, t = 0)}{\partial t} = 0,$$

$$\forall \underline{x} \in \Omega$$

$$\begin{cases} \dfrac{\partial u}{\partial x} \cos\theta + \dfrac{\partial u}{\partial z} \sin\theta - \sum_{j=1}^{p} \Psi_j = 0 \\ \forall (\underline{x}, t) \in \partial\Omega \times (0, \infty) \\ \dfrac{\partial \Psi_j}{\partial t} + 2\omega_j \Psi_j = \dfrac{\omega_j Y_j (Q)}{1 + \sum_{j=1}^{p} Y_j (Q)} \left(\dfrac{\partial u}{\partial x} \cos\theta + \dfrac{\partial u}{\partial z} \sin\theta \right) \\ \forall (\underline{x}, t) \in \partial\Omega \times (0, \infty) \quad j = 1, 2, \cdots, p \\ \Psi_j (\underline{x}, t = 0) = 0 \quad \forall \underline{x} \in \partial\Omega . \end{cases} \qquad (2.12)$$

Our model consists of the partial differential eq. (2.9) coupled with the system of ordinary differential eqs. (2.10) as well as the initial conditions (2.11) and the boundary conditions (2.12). The coupling of (2.9) and (2.10) with (2.12) represents the viscoelastic dynamics for heterogeneous dissipative media.

3. The finite-difference solution

Our initial boundary value problem (eqs. (2.9) through (2.12)) has to be solved for $\forall \underline{x} \in \Omega$, where Ω is an infinite domain because our medium is a heterogeneous half-space (see fig. 1). But because of the finite computer's core we can consider finite domains only; thus it is necessary to replace Ω by a finite domain, in such a way we can simulate the wave propagation in a heterogeneous half-space. For this aim it is necessary to introduce artificial boundaries into Ω. Let L_x, $L_z \in \Re$ and L_x, $L_z > 0$ be such that

$$L_z > \min_{0 < x < L_x} f(x)$$

and let

$$\Omega' = \{(x, z) \in \Re^2 \,|\, f(x) < z < L_z,\ 0 < x < L_x\}$$

be our finite domain with artificial boundaries

$$\begin{cases} \Gamma_1 = \{(0, z) \in \Re^2 ; \ f(0) < z < L_z\} \\ \Gamma_2 = \{(L_x, z) \in \Re^2 ; \ f(L_x) < z < L_z\} \\ \Gamma_3 = \{(x, L_z) \in \Re^2 ; \ 0 < x < L_x\}. \end{cases}$$

These boundaries must be equipped with artificial boundary conditions so that the perimeter of the computational grid becomes *transparent* to outward-moving waves in order to avoid artificial reflections introduced by the edges.

The transparent boundary conditions problem has not been solved at present, although it has been extensively studied (*e.g.*, Smith, 1974; Clayton and Engquist, 1977; Engquist and Majda, 1977; Reynolds, 1978; Sochacki

et al., 1987; Collino, 1993; Mei *et al.*, 1993). We have adopted Reynolds (1978) transparent boundary conditions which can be seen as a first-order approximation of the Engquist and Majda (1977) conditions.

To numerically solve our initial boundary value problem, we use eqs. (2.9) through (2.12) and the Reynolds (1978) transparent boundary conditions replacing Ω by Ω'. We use a finite-difference technique with a uniform mesh spacing in Ω'

$$h = \Delta x = \Delta z.$$

The choice of h depends on the frequency up to which the computation is required to be accurate

$$h = \frac{v_{\min}}{12 f_{\max}}$$

where $v_{\min}$ is the minimum wave velocity in Ω'. Let M and N be positive integers such that $M = \text{int}\left(\frac{L_x}{h}\right)$ and $N = \text{int}\left(\frac{L_z}{h}\right)$ and let

$$x_m = (m-1)\,h \qquad m = 1, 2, \cdots, M+1$$

and

$$z_n = (n-1)\,h \qquad n = 1, 2, \cdots, N+1.$$

The time step Δt must satisfy the Courant-Friedrichs-Lewy stability condition which, for the explicit finite-difference scheme that we use, is (see Mitchel and Griffiths, 1980)

$$\Delta t = \frac{h}{v_{\max}\sqrt{2}}$$

where $v_{\max}$ is the maximum wave velocity in the medium. Let

$$t_l = l\Delta t \qquad l = 1, 2, \cdots, J.$$

Then the interior mesh points are given by

$$\widehat{\Omega}_h = \{(x_m, z_n, t_l) \,|\, 2 \le m \le M,$$

$$2 \le n \le N, \quad 0 \le l \le J\}.$$

Let $u^l_{m,n}$, $\xi^l_{j,m,n}$, $\rho_{m,n}$, $\mu_{U,m,n}$, $\Psi^l_{j,m,n}$ and $G^l_{m,n}$ denote the finite difference-approximation of $u(x_m, z_n, t_l)$, $\xi_j(x_m, z_n, t_l)$, $\rho(x_m, z_n)$, $\mu_U(x_m, z_n)$, $\Psi_j(x_m, z_n, t_l)$ and $G(x_m, z_n, t_l)$, respectively. The discretization of the self-adjoint derivatives is written as

$$\nabla \cdot [\mu_U(x_m, z_n)\,\nabla u(x_m, z_n, t_l)] =$$

$$= \nabla \cdot \left[\frac{\mu_{U,m,n}}{h}\begin{pmatrix} u^l_{m+1,n} - u^l_{m,n} \\ u^l_{m,n+1} - u^l_{m,n}\end{pmatrix}\right] =$$

$$= \frac{1}{h^2}[E_{m+1}u^l_{m+1,n} - (E_{m+1}+E_m)\,u^l_{m,n} + E_m u^l_{m-1,n}] +$$

$$+ \frac{1}{h^2}[+F_{n+1}u^l_{m,n+1} - (F_{n+1}+F_n)\,u^l_{m,n} + F_n u^l_{m,n-1}]$$

where

$$E_m = \frac{1}{h}\left[\int_{(m-1)h}^{mh} \frac{dx}{\mu_U(\underline{x})}\right]^{-1}$$

$$F_n = \frac{1}{h}\left[\int_{(n-1)h}^{nh} \frac{dz}{\mu_U(\underline{x})}\right]^{-1}.$$

This approximation, first developed by Tikhonov and Samarskii (1961), allows us to save the self-adjoint nature of the operator $\nabla \cdot [\mu_U(\underline{x})\,\nabla u(\underline{x})]$ (see also Mitchell and Griffiths, 1980).

The discretization of (2.10) yields

$$\xi_j^{l+\frac{1}{2}} = A_j \xi^{l-\frac{1}{2}}_{j,m,n} +$$

$$+ B_j\left[\frac{\partial}{\partial x}\left(\frac{\mu_{U,m,n}Y_{j,m,n}}{1+\sum_{j=1}^{p}Y_{j,m,n}}\frac{\partial u}{\partial x}\right) + \right. \tag{3.1}$$

$$\left. + \frac{\partial}{\partial z}\left(\frac{\mu_{U,m,n}Y_{j,m,n}}{1+\sum_{j=1}^{p}Y_{j,m,n}}\frac{\partial u}{\partial z}\right)\right]_{t=l\Delta t}$$

$$j = 1, 2, \cdots, p$$

where

$$A_j = \frac{2 - \omega_j \Delta t}{2 + \omega_j \Delta t} \qquad B_j = \frac{2\,\omega_j \Delta t}{2 + \omega_j \Delta t}$$

$$j = 1, 2, \cdots, p.$$

Finally, the discretization of the wave eq. (2.9) gives

$$u^{l+1}_{m,n} = \frac{r^2}{\rho_{m,n}}(E_{m+1}u^l_{m+1,n} + E_m u^l_{m-1,n}) + \frac{r^2}{\rho_{m,n}}(F_{n+1}u^l_{m,n+1} + F_n u^l_{m,n-1}) + \left[2 - \frac{r^2}{\rho_{m,n}}(E_{m+1} + E_m + F_n + F_{n+1})\right]u^l_{m,n} - u^{l-1}_{m,n} + \frac{1}{\rho_{m,n}}G^l_{m,n} - \frac{(\Delta t)^2}{\rho_{m,n}}\sum_{j=1}^{p}\left(\frac{\xi^{l+\frac{1}{2}}_{j,m,n} + \xi^{l-\frac{1}{2}}_{j,m,n}}{2}\right) \tag{3.2}$$

for $m = 2, 3, \cdots, M$ $n = 2, 3, \cdots, N$ $1 < l < J - 1$, and $r = \frac{\Delta t}{h}$. We adopted the *leap frog* technique to discretize (2.10) in the time domain because it allows us to replace the value of ξ^l by the average of ξ-values at the time levels $l - 1/2$ and $l + 1/2$. Other choices lead to numerical instabilities as experienced in numerical experiments.

If we apply a stair-case on a regular grid, the discretization of the *stress-free dissipative* boundary condition (2.12) yields

$$u^l_{m+1,f_n}\cos\theta + u^l_{m,f_n+1}\sin\theta - u^l_{m,f_n}(\cos\theta + \sin\theta) - h\sum_{j=1}^{p}\left(\frac{\Psi^{l+\frac{1}{2}}_{j,m,f_n} + \Psi^{l-\frac{1}{2}}_{j,m,f_n}}{2}\right) = 0 \tag{3.3}$$

$$f(x_n) = f_n \in \partial\Omega$$

where the curve $f(x)$ is the free surface of the medium (see fig. 1), and the auxiliary unknown functions $\Psi^{l+\frac{1}{2}}_{j,m,f_n}$ are the solutions of the following system:

$$\begin{cases} \Psi^{l+\frac{1}{2}}_{j,m,f_n} = C_j\Psi^{l-\frac{1}{2}}_{j,m,f_n} + D_j\left(\dfrac{\partial u}{\partial x}\cos\theta + \dfrac{\partial u}{\partial z}\sin\theta\right)_{t=l\Delta t} \\ C_j = \dfrac{2 - \omega_j\Delta t}{2 + \omega_j\Delta t} \\ D_j = \dfrac{2\omega_j\Delta t Y_{j,m,f_n}}{(2 + \omega_j\Delta t)(1 + \sum_{j=1}^{p} Y_{j,m,f_n})} \\ j = 1, 2, \cdots, p \end{cases} \tag{3.4}$$

with initial conditions

$$\Psi^0_{j,m,f_n} = 0 \qquad j = 1, 2, \cdots, p.$$

Equations (3.1) through (3.4) are the finite-difference scheme for the vertical incidence.

Exactly the same scheme holds in the oblique incidence case: to take into account variations of the incident angle of the incoming plane wave, we rotate the 2D model reducing in such a way the oblique incidence to the vertical one. Let α be the angle between the incident direction and the normal to the x-axis. Let us introduce a coordinate system (x', z') in such a way that the incoming wave front is normal to the x' axis (see fig. 2a). If we rotate both the coordinate sytems clockwise by the angle α (see fig. 2b) we go back to the case of a vertical incidence. Let R be the operator of rotation defined as

$$R = \begin{pmatrix} \cos\alpha & \sin\alpha \\ -\sin\alpha & \cos\alpha \end{pmatrix}. \tag{3.5}$$

Ω' in the new coordinates x' and z' is

$$\Omega'_{\text{rot}}(x', z') = \Omega'\left(R^T\begin{pmatrix} x' \\ z' \end{pmatrix}\right) \qquad \forall (x', z') \in \Omega'_{\text{rot}} \tag{3.6}$$

where R^T is the transpose of R and the relations

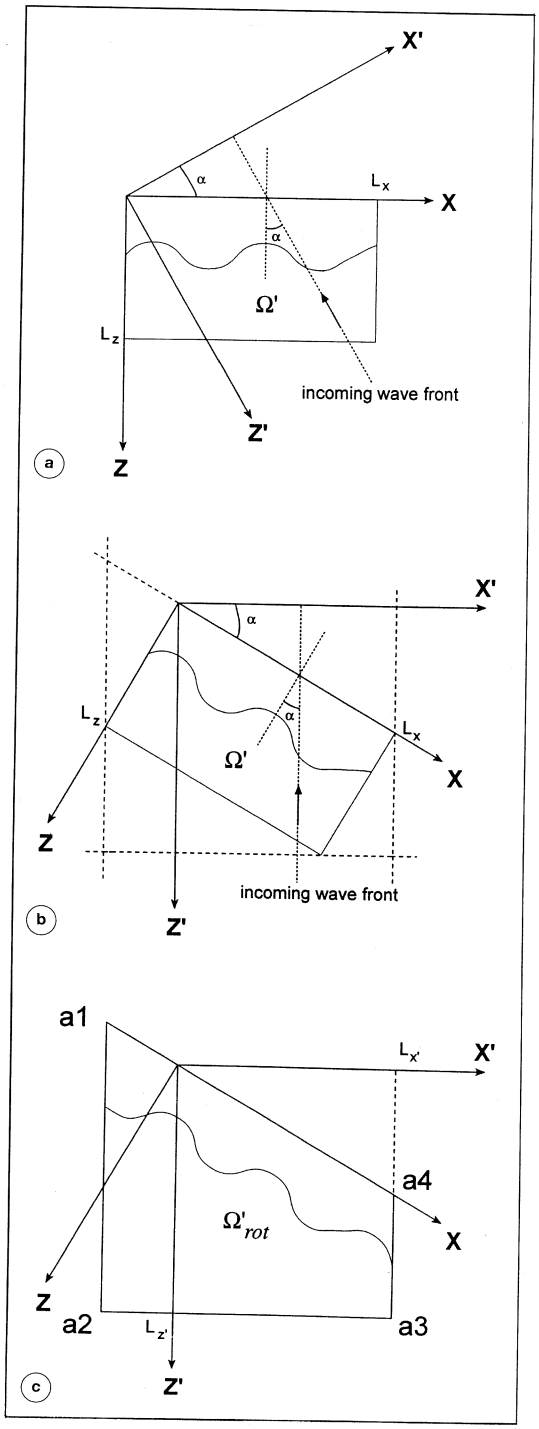

between new and old coordinates are

$$\begin{pmatrix} x' \\ z' \end{pmatrix} = R \begin{pmatrix} x \\ z \end{pmatrix} \quad \forall (x, z) \in \Omega' \quad \forall (x', z') \in \Omega'_{\text{rot}}. \tag{3.7}$$

The initial boundary value problem (2.9) through (2.12) is now solved in the new domain Ω'_{rot}, *i.e.* in the trapetium (a_1, a_2, a_3, a_4) sketched in fig. 2c. The coordinates (x, z) do not play any role in the numerical computation for oblique incidence, we need them just to rotate Ω' via relations (3.5), (3.6) and (3.7).

4. Numerical tests

In order to check the suitability of our numerical code, we used the same 2D geological structure modelled by Moczo *et al.* (1995). Figure 3 shows the geological model including elastic and anelastic parameters of the different layers. A first test deals with the vertical incidence.

The computational section is 982 m wide and 117 m deep. We used the same time-step (0.00039 s) as in Moczo *et al.* (1995), and the smallest grid-step (0.5 m) employed by Moczo *et al.* (1995) in his variable grid model. These parameters guarantee the accuracy of the finite-difference computation up to 15 Hz. The input radiation in this case is represented by a vertically incident planewave. To realize such

Fig. 2a-c. Three steps are needed to realize the oblique incidence. a) The wave front is incident with an angle α in the (x, z) frame. Note that in the (x', z') frame the wave front has a vertical incidence $(\alpha = 0)$. b) Both coordinate frames and the Ω' domain are rotated clockwise by the angle α. c) The rotated Ω'_{rot} domain (the trapezium a_1, a_2, a_3, a_4,) is the new domain of integration for the same initial boundary value problem (2.9) through (2.12).

	VELOCITY [m/s]	DENSITY [kg/m³]	Q FACTOR
1	400	1900	40
2	100	1800	15
3	400	1900	40
4	800	2050	100

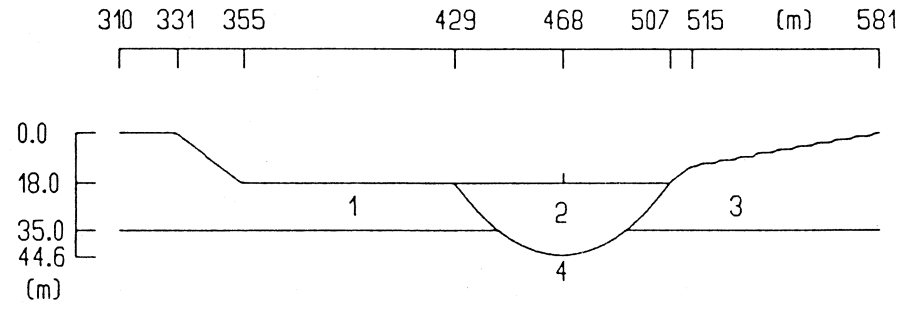

Fig. 3. 2D vertical section with table of elastic and anelastic parameters used in the numerical tests. The entire profile used in the computation is 982 m long and 117 m deep. Geometry and mechanical parameters are the same as in Moczo *et al.* (1995).

an input radiation we use the Gabor impulse

$$g(t) = \exp\left[-\left(\frac{\omega_p (t-t_s)}{\gamma}\right)^2\right] \cos\left[\omega_p (t-t_s) + \psi\right] \tag{4.1}$$

where $\omega_p = 2\pi f_P$, $t_s = 0.45\,\gamma/f_P$. f_P is the predominan frequency of the impulse. The parameter values in our modelling were equal to those used in Moczo *et al.* (1995). Figure 4a,b shows the comparison between the results of our modelling and the previous one as published in Moczo *et al.* (1995). The propagation pattern does not show any significant difference between the two results. To evaluate the size of differences in the spectral content, three representative sites were selected within the soft upper layer, one in the middle of the valley and two close to the edges. For these sites Fourier transfer functions were estimated through the spectral ratios between the synthetic seismograms at the surface and the bedrock input (see fig. 5). The details of the spectral content are precisely reproduced and the maximum deviation at specific frequencies does not exceed 5%. These satisfactory results validate our numerical code.

The second test case deals with plane-wave oblique-incidence. We rotated the structure sketched in fig. 3 using the technique explained in the previous paragraph. Elastic and anelastic parameters as well as grid and time steps are the same as those used in the vertical incidence case. Figure 6 shows synthetic displacement on the free surface for an incoming plane wave with an angle $\alpha = 30°$ measured from the x axis in the clockwice direction. It is noteworthy that, compared to the vertical incidence case, waves trapped inside the horizontal

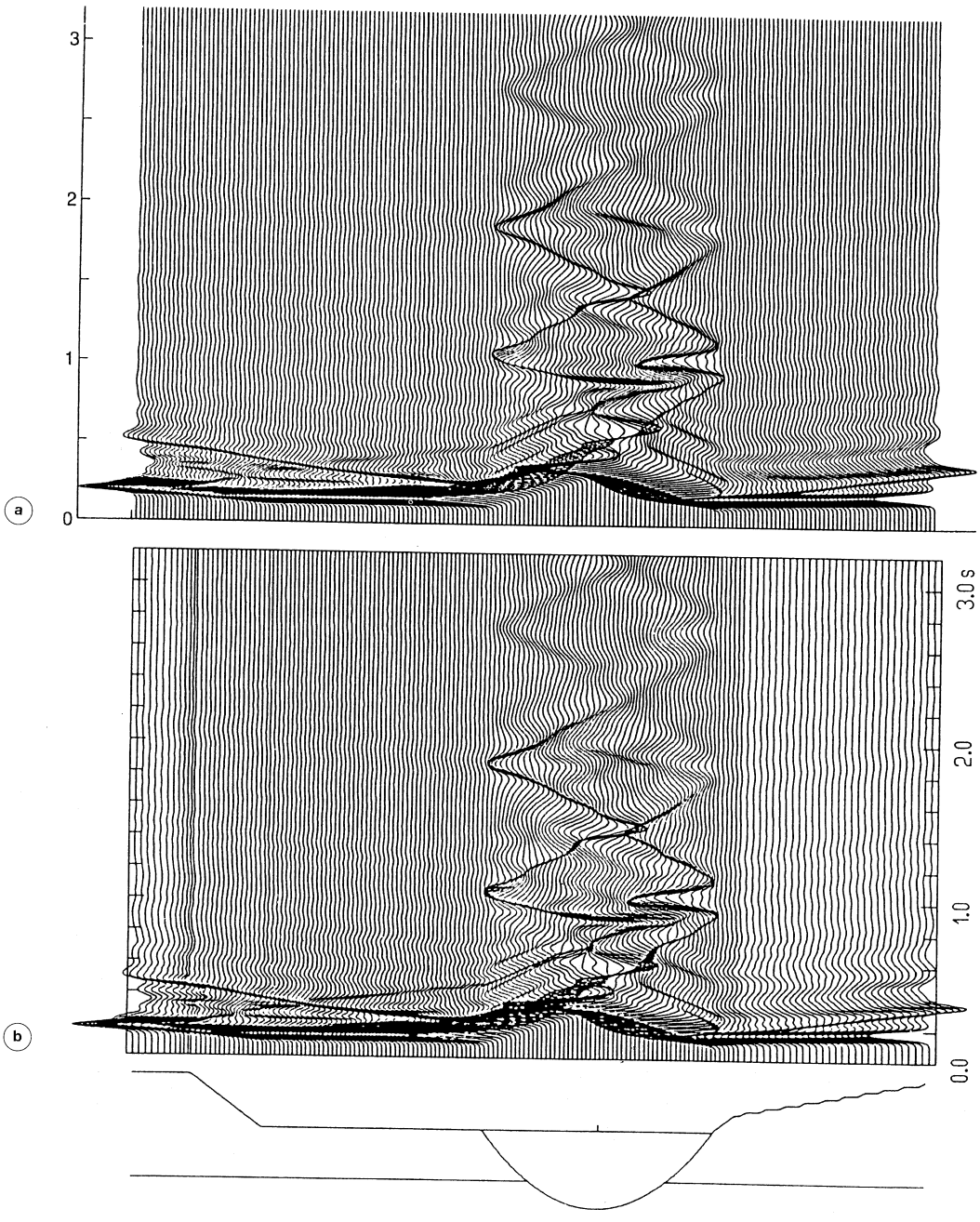

Fig. 4a,b. Comparison between synthetic displacement on the free surface derived from (a) our computation and (b) Moczo *et al.* (1995). In (a), the same *delta-like* input of Moczo *et al.* (1995) was used.

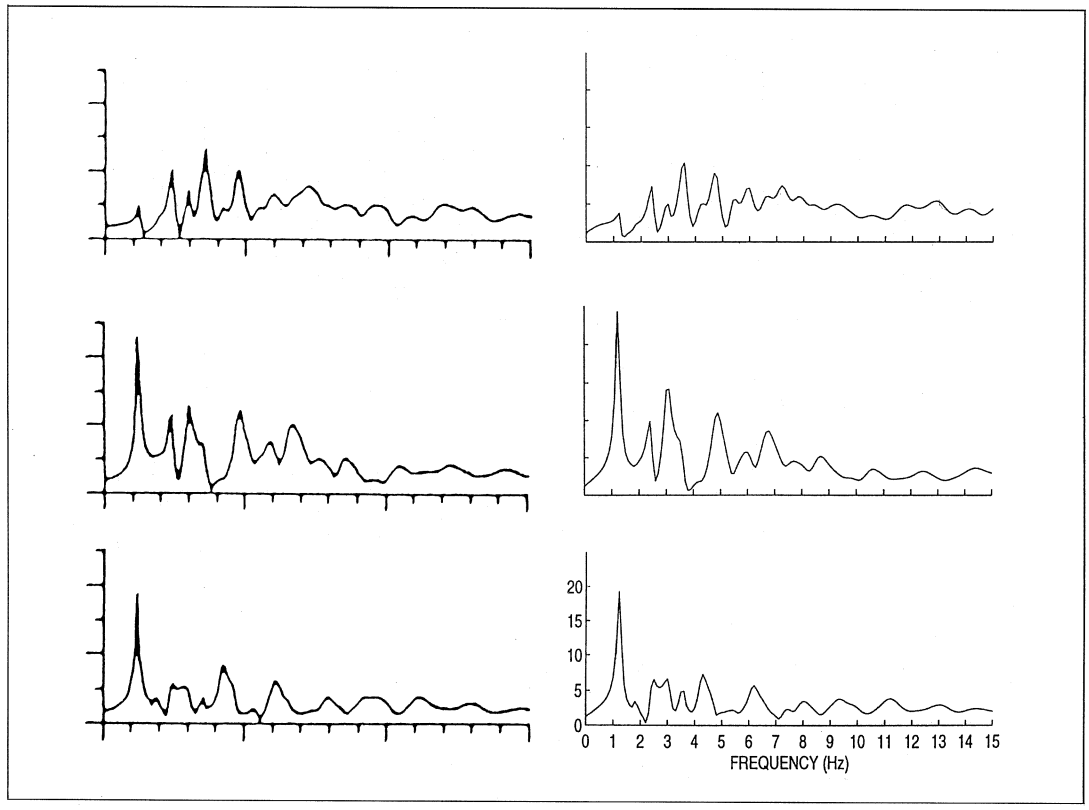

Fig. 5. Comparison between our Fourier transfer functions (right column) and the Moczo *et al.* (1995) ones (left column) for three sites in the valley. The sites are at $x = 438$ m (top), $x = 468$ m (middle) and $x = 480$ m (bottom), respectively. The x coordinates are according to fig. 3.

layer on the right hand-side of the profile provide the valley with energy. This generates more complicated interference effects in the valley.

When a real geological structure is taken into account, the complex interfaces of the input model are automatically digitized according to the stability conditions of the numerical scheme. Figure 7 shows an example of a real 2D vertical section of a geological profile in Rome, Italy. Interfaces were digitized after grouping different geological layers on the basis of similar mechanical properties (fig. 8). The transient response of this real structure to a vertically incident pulse is shown in fig. 8. The bedrock input was the Gabor function as defined in (4.1). The time and grid steps are those used in the test cases of figs. 4a,b and 6.

5. Conclusions

In this study we present a numerical model to solve the viscoelastic dynamics of antiplane wave propagation in a 2D heterogeneous dissipative medium with nonplanar free surface both for vertical and oblique incidence. Input at the bedrock is an out-of-plane polarized wave. An initial boundary value problem is formulated to represent a dissipative dynamics

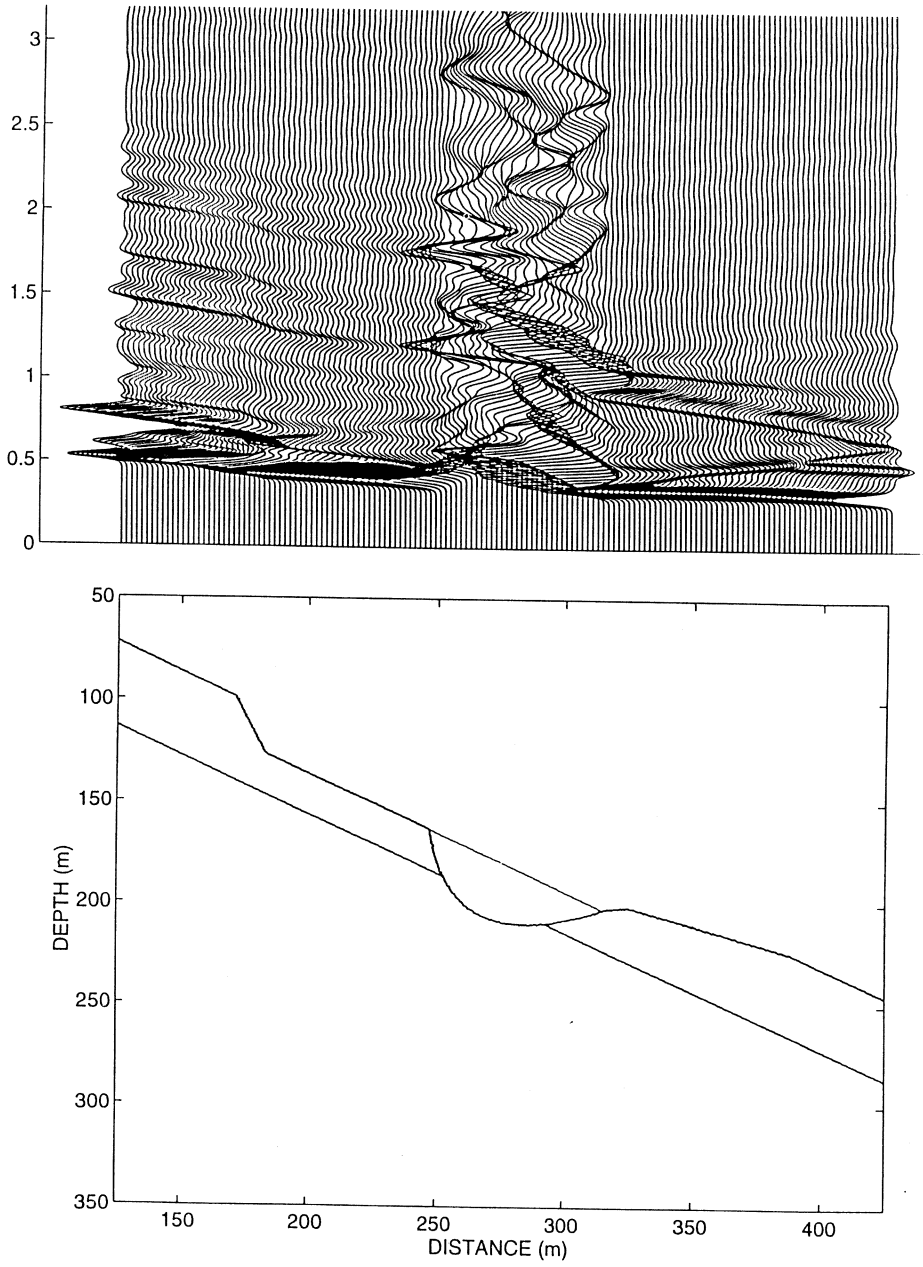

Fig. 6. Transient response of the model for an obliquely incident wavefront with an angle of 30° degrees. The input radiation is the same *delta-like* signal as in the vertical case. The entire profile used in the computation is 563 m long and 427 m deep.

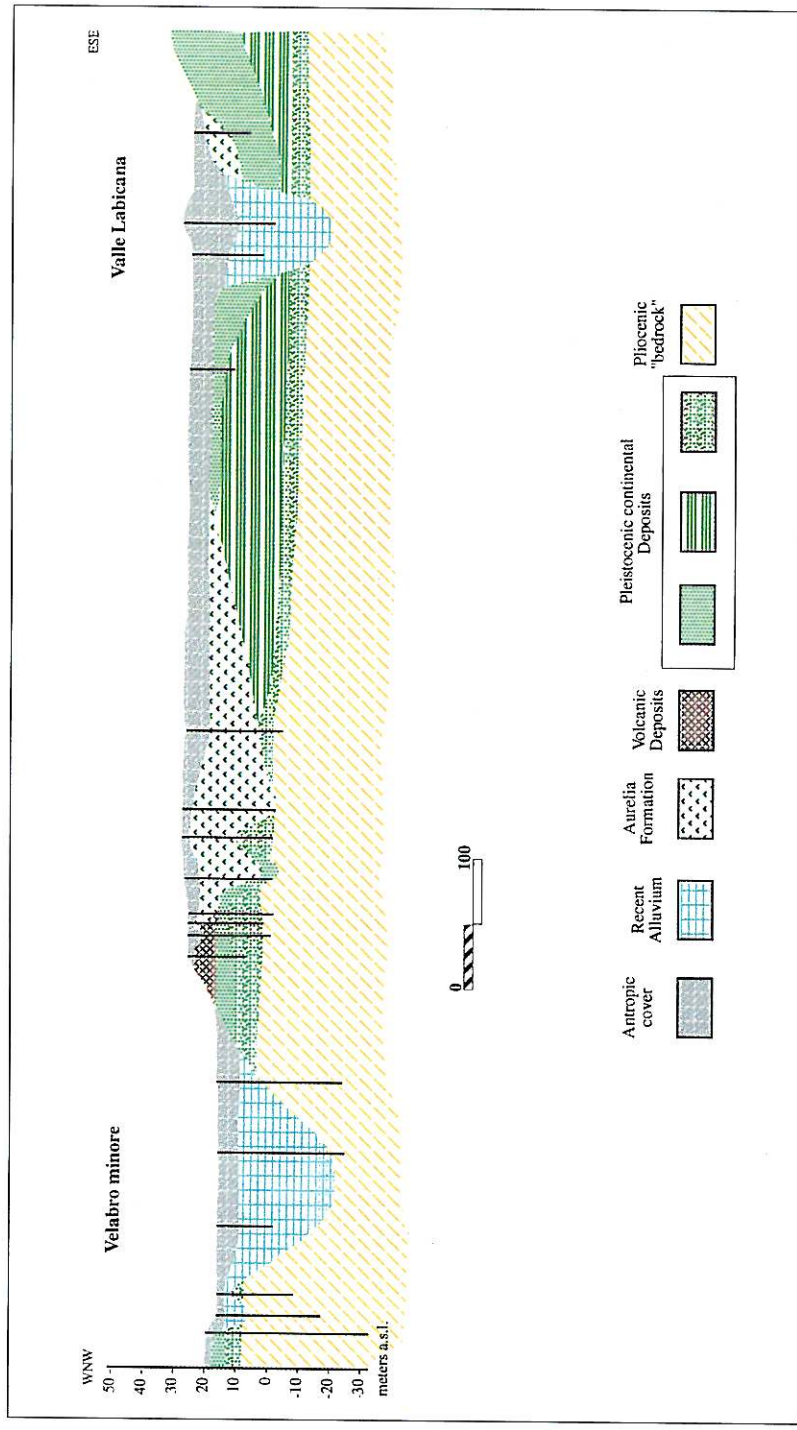

Fig. 7. This 2D vertical section is a real WNW-ESE oriented profile in the historical centre of the city of Rome. It includes two alluvium-filled basins connected by different geological layers. The site is characterized by irregular topography. The vertical black lines are boreholes drilled in the area to study the stratigraphy of the city.

Geological Units	S Velocity m/s	Density g/cm^3	Q factor
1: Antropic Cover	100	1.85	10
2: Recent Alluvium	200	1.85	10
3: Continental Deposits	400	1.95	20
4: Pliocenic "Bedrock"	800	2.0	50

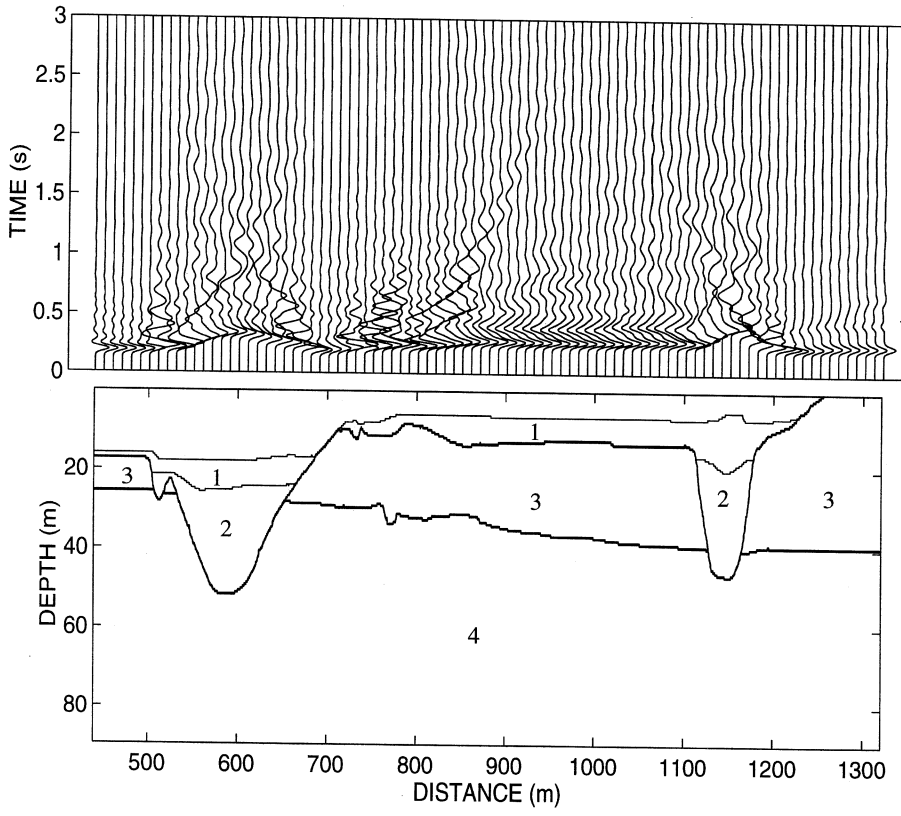

Fig. 8. A digitized geological profile is reconstructed after grouping different geological units on the basis of their mechanical properties (1: manmade fillings; 2: recent alluvium; 3: continental and volcanic deposits; 4: Pliocenic bedrock). The site response to a vertically incident plane wave is shown together with the elastic and anelastic parameters used in the modelling.

in realistic 2D geological profiles. The mathematical formulation of the wave propagation problem includes the forcing term which provides the initial perturbation. Its discretization numerical scheme is based on a finite-difference technique. We adopted the rheological Maxwell body model to take into account absorption mainly for two reasons. First, it allows us to directly compute the dissipated solution in the time domain: this means that no artifices, like low-pass filters, are needed in order to simulate the absorption effects. Second, because of its superiority both in accuracy and in computational efficency. The numerical scheme is structured to model the vertical incidence. A comparison with previously published results guarantees the suitability of this code. Rotating the 2D model we reduce the oblique incidence to the vertical one. The advantage of this technique is that no variations are needed in the numerical scheme to account for angle variations of the incident wave front. In this way we are guaranteed that no errors are introduced with respect to the vertical incidence case.

Acknowledgements

I am grateful to Francesco Zirilli for his help in the early stage of this work. Many discussions with Jiri Zahradnik, Peter Moczo and Antonio Rovelli were very useful throughout the work development. Thanks are due to Dave Boore and Francisco Sáncez-Sesma for their critical review of the paper. I wish to express my gratitude to Enzo Boschi for his interest and encouragement.

REFERENCES

BARD, P.-Y. (1995): Effects of surface geology on ground motion: recent results and remaining issues, in *Proceeedings of the 10th European Conference on Earthquake Engineering*, August 28 September 1994, Vienna, Austria (Gerald Duma Editor), vol. 2, 305-324.

BARD, P.-Y. and M. BOUCHON (1980): The seismic response of sediment-filled valleys. Part 1. The case of incident SH waves, *Bull. Seism. Soc. Am.*, **70**, 1263-1286.

BOORE, D.M. (1972): Finite-difference methods for seismic waves, in *Methods in Computational Physics*, edited by B.A. BOLT (Academic Press, New York), vol. 11, 1.-37.

CLAYTON, R. and B. ENGQUIST (1997): Absorbing boundary conditions for acoustic and elastic wave equations, *Bull. Seism. Soc. Am.*, **67**, 1529-1540.

COLLINO, F. (1993): High order absorbing boundary conditions for wave propagation models: straight line boundary and corner case, in *Second International Conference on Mathematical and Numerical Methods of Wave Propagation*, edited by R. KLEINMAN, T. ANGELL, D. COLTON, F. SANTOSA, I. STAKGOLD, *SIAM Proceedings Series, Philadelphia*, 161-171.

EMMERICH, H. and M. KORN (1987): Incorporation of attenuation into time-domain computations of seismic wave fields, *Geophysics*, **52**, 1252-1264.

ENGQUIST, B. and A. MAJDA (1997): Absorbing boundary conditions for the numerical simulation of waves, *Math. Comp.*, **31**, 629-651.

MEI, K.K., R. POUS, Z. CHEN, Y.W. LIU and M.D. PRONTY (1993): Measured equation of invariance: a new concept in field computations, *IEEE Trans. Antennas Propag.*, **42**, 320-328.

MITCHEL, A.R. and D.F. GRIFFITHS (1980): *The Finite Difference Method in Partial Differential Equations* (John Wiley & Sons, New York).

MOCZO, P. (1989): Finite-difference technique for *SH*-waves in 2D media using irregular grids – application to seismic response problem, *Geophysics*, **99**, 321-329.

MOCZO, P. and P. BARD (1993): Wave diffraction and differential motion near strong lateral discontinuities, *Bull. Seism. Soc. Am.*, **83**, 85-106.

MOCZO, P., A. ROVELLI, P. LABÁK and L. MALAGNINI (1995): Seismic respose of the geological structure underlying the Roman Colosseum and a 2D resonance of a sediment valley, *Ann. Geofis.*, **38** (5-6), 939-956.

PADOVANI, E., E. PRIOLO and G. SERIANI (1995): Low and high-order Finite Element Method (FEM): experience in seismic modeling, *J. Comp. Acoustic*, **28**, 845-885.

REYNOLDS, A.C. (1978): Boundary conditions for the numerical solution of wave propagation problems, *Geophysics*, **43**, 1099-1110.

SÁNCHEZ-SESMA, F.J. and M. CAMPILLO (1991): Diffraction of *P*, *SV*, and Rayleigh waves by topographic features: a boundary integral formulation, *Bull. Seism. Soc. Am.*, **81**, 2234-2253.

SMITH, W.D. (1974): A nonreflecting plane boundary for wave propagation problems, *J. Comp. Phys.*, **15**, 492-503.

SOCHACKI, J., R. KUBICHEK, J. GEORGE, W.R. FLETCHER and S. SMITHSON (1987): Absorbing boundary conditions and surface waves, *Geophysics*, **52**, 60-71.

TIKHONOV, A.N. and A.A. SAMARKII (1961): Homogeneous difference schemes, *Z. Vycisl. Mat. i Mat. Fiz.*, **1**, 5-63.

ZAHRADNIK, J. (1995): Simple elastic finite-difference scheme, *Bull. Seism. Soc. Am.*, **85**, 1879-1887.

ZAHRADINK, J. and E. PRIOLO (1995): Heterogeneous formulations of elastodynamic equations and finite-difference schemes, *Geophys. J. Int.*, **120**, 665-676.

ZAHRADNIK, J., P. MOCZO and F. HRON (1993): Testing four elastic finite-difference schemes for behaviour at discontinuitites, *Bull. Seism. Soc. Am.*, **83**, 107-129.

(received May 2, 1998;
accepted September 23, 1998)

Appendix

The stress-strain relations including dissipation are (Emmerich and Korn, 1987):

$$\begin{cases} \sigma_{yx} = 2\mu_U \left(\frac{1}{2} \frac{\partial u}{\partial x} - \sum_{j=1}^{p} \zeta_{j,\,yx} \right) \\ \sigma_{yz} = 2\mu_U \left(\frac{1}{2} \frac{\partial u}{\partial z} - \sum_{j=1}^{p} \zeta_{j,\,yz} \right) \end{cases} \tag{A.1}$$

In (A.1), the tensors $\zeta_{j,\,yx}(\underline{x}, t)$ and $\zeta_{j,\,yz}(\underline{x}, t)$ $j = 1, 2, \cdots, p$ are the anelastic terms of the stress-strain relation and satisfy the system:

$$\begin{cases} \frac{\partial \zeta_{j,\,yx}}{\partial t} + \omega_j \zeta_{j,\,yx} = \frac{1}{2} \left(\frac{\omega_j Y_j}{1 + \sum_{j=1}^{p} Y_j} \right) \frac{\partial u}{\partial x} & j = 1, 2, \cdots, p \\ \frac{\partial \zeta_{j,\,yz}}{\partial t} + \omega_j \zeta_{j,\,yz} = \frac{1}{2} \left(\frac{\omega_j Y_j}{1 + \sum_{j=1}^{p} Y_j} \right) \frac{\partial u}{\partial z} & j = 1, 2, \cdots, p \end{cases} \tag{A.2}$$

where ω_j are the relaxation frequencies and the coefficients Y_j ($j = 1, 2, \cdots, p$) are the weight factors of the classical Maxwell bodies constituting the generalized Maxwell body. They are the solution of the linear system (Emmerich and Korn, 1987):

$$\sum_{j=1}^{p} \frac{\tilde{\omega}_k \left[\omega_j - Q^{-1}(\underline{x}, \tilde{\omega}_k)\, \tilde{\omega}_k \right]}{\omega_j^2 + \tilde{\omega}_k^2} Y_j = Q^{-1}(\underline{x}, \tilde{\omega}_k) \qquad k = 1, \cdots, K. \tag{A.3}$$

Inserting (A.1) in (2.1), we have the partial differential equation of wave propagation:

$$\rho \frac{\partial^2 u}{\partial t^2} = \frac{\partial}{\partial x} \left(\mu_U \frac{\partial u}{\partial x} \right) + \frac{\partial}{\partial z} \left(\mu_U \frac{\partial u}{\partial z} \right) - \sum_{j=1}^{p} \zeta_j + G(\underline{x}, t) \tag{A.4}$$

where the functions $\xi_j(\underline{x}, t)$ are defined as

$$\xi_j = 2 \left[\frac{\partial}{\partial x} (\mu_U \zeta_{j,\,yx}) + \frac{\partial}{\partial z} (\mu_U \zeta_{j,\,yz}) \right] \qquad j = 1, 2, \cdots, p. \tag{A.5}$$

In order to find the equations whose solutions are the auxiliary unknown functions ξ_j, we consider the system (A.2). We multiply by $2\mu_U$ the first and second equation, differentiating the first equation with respect to x and the second one with respect to z, summing them up, and taking into account definition (A.5) we get the equations whose solutions are the auxiliary unknown functions ξ_j, *i.e.* eq. (2.2) in the text.